

# Investigating White Matter Perfusion using Optimal Sampling Strategy Arterial Spin Labeling (OSS-ASL) at 7T

Alexander Graeme Gardener<sup>1</sup> and Peter Jezzard<sup>1</sup>

<sup>1</sup>FMRIB Centre, Nuffield Department of Clinical Neurosciences, Oxford, United Kingdom

**Introduction:** The investigation of White Matter (WM) perfusion (CBF) by Arterial Spin Labeling (ASL) techniques has proven to be challenging, mainly due to the low intrinsic difference signal ( $\Delta M$ ) between the control and labeled images, which limits the Contrast-to-Noise ratio (CNR) obtainable. From the literature the WM  $\Delta M$  signal is reported to be approx. 2-4 times smaller than Grey Matter (GM)  $\Delta M$ , with arterial transit times also longer, leading to increased relaxation (and signal loss) of labeled blood before arrival and perfusion into the tissue. Recent studies have implemented developments in labeling sequences such as higher CNR pseudo-Continuous ASL, to assess how increasing averages of single delay time (TI) image pairs improves CNR<sup>1</sup>, or by combining multiple TI pCASL with fine detail ROI analysis<sup>2</sup>. Further, single WM large-voxel acquisition has been suggested to overcome the WM CNR limitation<sup>3</sup>. There are also concerns over partial voluming between WM and GM that could lead to over-estimation of WM CBF<sup>4</sup>. With the increasing availability of ultra-high field human scanners we can take advantage of both higher CNR and longer T1 blood relaxation time in order to improve WM ASL acquisition. Coupled with an Optimal Sampling Strategy (OSS) approach, used to improve selection of TI times for WM in real-time<sup>5</sup>, we aimed to optimize ASL image acquisition for WM CBF quantification.

**Methods:** Scanning was performed using a 7T Siemens scanner, equipped with a 32 channel receive, and single-channel transmit, coil. The physical extent of this coil, combined with ultra-high field B<sub>1</sub> profile and efficiency issues, led to employing a FAIR-QUIPSS2 based pulsed ASL sequence for the study<sup>6</sup>. Inversion (FOCI) and saturation (SLR-optimized) pulse efficiencies were assessed in a phantom (T1=1400ms) and were >95% at  $\pm 8$ cm from field iso-centre. The initial TI<sub>2</sub> search space ranged 0.8-2.55 seconds, evenly spaced across 8 TI<sub>2</sub>s. OSS was then used to iteratively improve the TI<sub>2</sub> distribution for subsequent blocks of control-tag acquisitions, in real-time<sup>5</sup>. Following each block acquisition (i.e. 8 pairs of control-tag images), a direct search algorithm (used for high processing speed) ran in the image-processing pipeline on the reconstruction computer. This optimized standard ASL general kinetic model<sup>7</sup> parameters on a masked voxel-by-voxel basis; best-fitted voxel  $\Delta M$  time-courses; binned distribution of optimal TI<sub>2</sub>s from fits; and in real-time fed-back to the scanner a new set of TI<sub>2</sub>s to be subsequently acquired, in <1 second of processing. The process then repeated with all data collected thus far included in the next OSS run, to iteratively generate an ever-improving TI<sub>2</sub> set. Convergence of TI<sub>2</sub>s to overall optimized values is therefore achieved. For this study double inversion recovery (DIR) prepared images were acquired prior to ASL scans to generate the masks for OSS, thresholding DIRs as part of image recon. Two approaches were used; A) WM-weighted image alone, and B) WM- minus GM-weighted images. Representative DIR and masks are shown in Figure 1. Scans had resolution of 3x3x5mm<sup>3</sup> for a 64<sup>2</sup> matrix and six axial slices, spacing 2mm, ascending order, positioned with bottom slice on top of ventricles. Gradient-echo EPI with 6/8 partial Fourier was used, with flow crushers in the z-direction at critical velocity 5cm/s. FAIR ASL acquisition applied QUIPSS2 saturation at 0.7s post-inversion (TI<sub>1</sub>), whilst pre- and post-inversion slice saturation were used; TE was 18ms and ASL TR was 4s [ $\sim 95\%$  SAR limit at 7T]. Effective gap between tag and first slice was 20mm. For each ASL scan 160 images (10 blocks) were acquired ( $\sim 11$  minutes total) for five healthy adult male subjects (ages 35 $\pm$ 4 years). One subject also had an OSS-ASL scan using a GM mask to compare TI<sub>2</sub> distributions.

An unprepared M<sub>0</sub> image was acquired for CBF quantification. Post-acquisition, data were taken offline and post-processed using FSL tools<sup>8</sup>. Matlab [Mathworks, MA] was used to prepare  $\Delta M$  time-series (each  $\Delta M$  at different TI<sub>2</sub>) and FSL-BASIL then performed fast Bayesian fitting to the ASL kinetic model on the time-series. Later slice acquisition time delay to TI<sub>2</sub>, and different tissue T<sub>1</sub>s, were accounted for in the fitting. Processing from raw images to final CBF maps could be performed in <5 minutes. Tissue CBF values were analyzed using ROIs generated from DIR images, with voxels found in both ROIs discarded. BASIL-generated z-stats for WM CBF were used as a mark of goodness-of-fit.

**Results:** Table 1 shows CBF values for GM- and WM-only ROIs (averaged for slices and subjects);

WM (2) CBF is for WM voxels with CBF z-stat >2, which across subjects was found to be 75 $\pm$ 10% of WM-classed voxels. The ratio of GM to WM (2) CBF was found to be on average 2.9:1. Tissue BAT (Bolus Arrival Time) values are given for a single slice. Figure 2 presents CBF maps for 3 slices. Figure 3 plots OSS TI<sub>2</sub> distributions (last block, averaged across subjects) showing longer TI<sub>2</sub>s preferred for WM and WM-GM voxel masks, reflecting later arrival of labeled blood to these regions. There was significant difference between WM and GM, and WM-GM and GM, TI<sub>2</sub> distributions (p<0.01).

**Conclusion:** It has been shown it is possible to obtain reasonable CBF fits for WM at 7T using an OSS FAIR-QUIPSS2 sequence, in approx. 15 minutes of acquisition including preparation scans. Tissue CBF and BAT values are comparable to literature, with WM CBF slightly lower than previous studies, reflecting care in selecting voxels. The ratio of GM:WM CBF is also consistent with the literature. Future work will investigate higher resolution and applicability to WM disease studies.

## References

- 1 - van Osch, MRM, 2009.      2 - Lu, ISMRM, 2009.      3 - Pohmann, MRM, 2010.      4 - van Gelderen, MRM, 2008.  
5 - Xie, MRM, 2010.      6 - Gardener, MRM, 2009.      7 - Buxton, MRM, 1998.      8 - FSL ( <http://www.fmrib.ox.ac.uk/fsl/> ).



Figure 1: DIR WM, GM images; WM mask; WM-GM mask.

GM CBF	49 $\pm$ 13 ml/100g/min
WM (1) CBF	14 $\pm$ 1 ml/100g/min
WM (2) CBF	17 $\pm$ 2 ml/100g/min
GM BAT	0.76 $\pm$ 0.09 seconds
WM (1) BAT	0.91 $\pm$ 0.06 seconds
WM (2) BAT	0.96 $\pm$ 0.07 seconds

Table 1: Averaged tissue CBF and BAT.

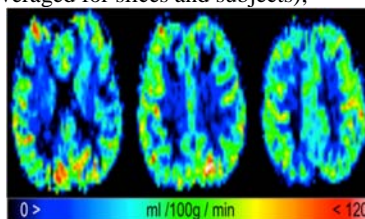


Figure 2: CBF maps for bottom 3 slices

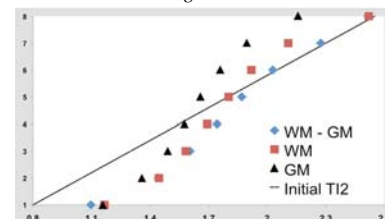


Figure 3: Plots of OSS last-block TI<sub>2</sub>s.